# EXPERIMENTS WITH ALUMINUM BONDED $Nb_3Sn$*

C. D. Henning, R. L. Nelson, H. L. Leichter, and C. O. Ward
Lawrence Livermore Laboratory, University of California
Livermore, California 94550

## Abstract

Experiments with $Nb_3Sn$ tapes have shown that adiabatic stability is relatively unchanged by bonding aluminum rather than copper to a superconductor. In the cusp coil configuration with edge cooling, test magnets of 0.5-in.-wide tape underwent a super-to-normal transition when the perpendicular fields reached 19 kG. Operation in superfluid helium increased the allowable perpendicular field to 23 kG. When connected in a solenoid configuration the conductors closely approached short sample performance. All tests were reproducible and somewhat sensitive to charging rate. Face cooling increased the coil performance to the cryogenic stability limit and decreased rate sensitivity. It is concluded that aluminum is best used for nucleate boiling stabilization in conjunction with face cooling. Measurements of the bearing strength of high-purity aluminum indicate that stresses greater than 8000 psi are permissible under insulation strips. Tensile strengths were measured and a model formulated for design and fracture loads.

## Introduction

The next generation of mirror magnets for controlled thermonuclear fusion will require that superconductors operate reliably with high current density in fields greater than 100 kG. The $Nb_3Sn$ compound is known to serve this function well in a solenoid, if there is no conductor movement and the magnetic field is nearly parallel to the conductor face. Unfortunately, unusual mirror magnet configurations, such as Baseball,[1] cannot easily satisfy these two conditions. The magnetic field is nearly perpendicular to the face of a strip conductor and some looseness on the winding is inevitable. Sufficient copper to cryogenically stabilize the superconductor would make the current density too low. Accordingly, a program was initiated to investigate the properties of $Nb_3Sn$ bonded to high-purity aluminum. The lower resistivity of aluminum might make cryogenic stability possible at useful current densities or at least improve dynamic stability. For strength, structural materials were bonded to the conductors. The superconducting $Nb_3Sn$ was manufactured by the diffusion process[2] in a variety of configurations with aluminum and stainless[3] steel.

## Stability

The first conductor tested had one 0.001-in. layer of $Nb_3Sn$ with a 0.005-in. layer of aluminum on one side and 0.004 in. of stainless steel on the other. Short sample measurements of the critical current were 950 A at 60 kG and 517 A at 100 kG. An aluminum resistivity ratio of 1400 was estimated by comparing the resistivity of the bonded conductor in liquid hydrogen to the resistivity of unbonded aluminum at liquid hydrogen and helium temperatures. Winding the conductor with a 0.005-in.-thick Mylar tape interleaving produced an eight pancake coil that had a 2-in. i.d. and a 4.5-in. o.d. Perforated epoxy-glass laminate was used between layers. Pancake connections were made so that the magnet could be operated as a solenoid or as a cusped pair. This cusped configuration, similar to that used at ORNL,[3] produces a high radial field at the magnet midplane and provides the most severe conditions for stability.

Because of the low resistivity of aluminum, greater adiabatic stability was expected than when the $Nb_3Sn$ was bonded to copper. However, Fig. 1 indicates that the performance was not improved. While the solenoids closely approached the short sample current, the cusped coils exhibited considerable degradation. Even at slow charging rates,

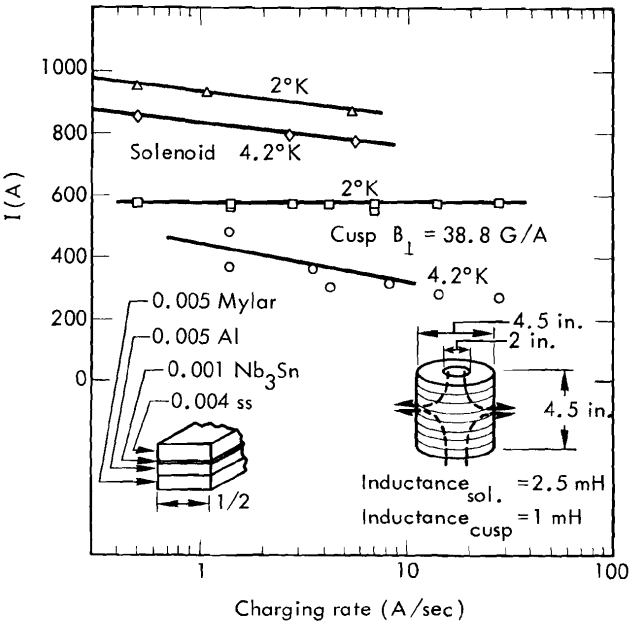


Fig. 1. Adiabatic stability of aluminum bonded $Nb_3Sn$.

*This work was performed under the auspices of the United States Atomic Energy Commission.

the first gross flux jump occurred at a perpendicular field of 18.6 kG and caused the coil to undergo a super-to-normal transition. The value is slightly less than the maximum perpendicular field of 25 ± 5 kG observed for copper-clad $Nb_3Sn$.[3,4]

Operation in superfluid helium did not greatly improve the stability, except for making the coil less rate sensitive. The maximum perpendicular field increased to 22.5 kG, probably because the higher current density delayed the collapse of the diamagnetic loop currents. The low dynamic stability of aluminum-bonded superconductors might have been anticipated from solutions to Bean's critical state model.[5] A change in perpendicular field $\Delta H_\perp$ induces a diamagnetic current loop at the critical current density ± Jc along the edge of a superconducting strip. It is possible to find the triangular flux penetration δ from Maxwell's equation:

$$\delta = \frac{\Delta H_\perp}{(4\pi/10)Jc} .$$

Swartz and Bean[6] analyzed the thermal instability caused by such a flux penetration and predicted, from an adiabatic model, that the first flux jump would occur at a given perpendicular field $H_\perp$ as a function of heat capacity C and the rate of change of current density Jc with temperature T:

$$H_\perp = \left[\pi^3 \cdot 10^7 \cdot C\left(-\frac{1}{Jc}\frac{\partial Jc}{\partial T}\right)^{-1}\right]^{1/2}$$

The heat capacity of aluminum is slightly less than that of copper (Table I). Hence, no improvement is expected. However, Hart[7] and Hancox[8] derive similar relationships for a quasiadiabatic model:

$$H_\perp^2 < \pi^2 K\, To/4\rho,$$

where the thermal conductivity K and the resistivity ρ of the substrate are considered. The symbol To is a characteristic temperature around 10°K. Since aluminum has a much lower resistivity than moderate-purity copper and about the same thermal conductivity, some improvement in dynamic stability was expected. It may be that the bond between the aluminum and $Nb_3Sn$ is not sufficiently conducting to achieve this advantage. Certainly from Fig. 2 one can see voids in the solder bond, and indeed the aluminum oxide layer may be sufficient to greatly degrade the bond. Measurements of the electrical and thermal conductivity of these bonds have not yet been attempted.

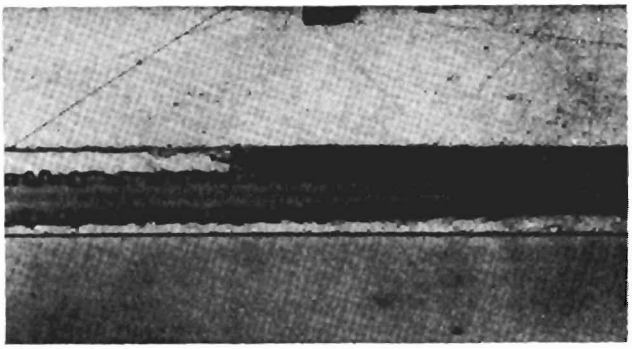

Fig. 2. Photomicrograph showing voids in solder bonds.

As an alternative, cryogenic stabilization was investigated by removing the Mylar interleaving each 0.5 in. and leaving a 0.25-in. gap for face cooling. The results (Fig. 3) show slightly improved performance. The magnet was only slightly rate sensitive, especially in superfluid helium, but went normal at the cryogenic stability limit of 0.2 W/cm$^2$. From the work by James, Lewis, and Maddock (Fig. 4) this is a reasonable heat flux in such restricted passages.[9] Little heat could be removed from the stainless steel-clad side of the conductor because of the very low thermal conductivity. Also, there was some concern that the energy stored in the diamagnetic currents would release suddenly with a flux jump, causing a transition from nucleate-to-film boiling. Then it would be necessary to design for the recovery rather than the peak nucleate-boiling heat flux. From the self-inductance of a strip conductor,[10] the

TABLE I. Heat Capacity of Low Resistivity Metals

| Metal | Density g/cm$^3$ | Heat capacity, $C_p$ J/g°K 2°K | 4°K | Heat capacity, C J/cm$^3$°K 2°K | 4°K | $C/C_{cu}$ 4°K |
|---|---|---|---|---|---|---|
| Aluminum | 2.7 | 0.000108 | 0.000261 | 0.000291 | 0.000705 | 0.86 |
| Copper | 8.96 | .000028 | .000091 | .000250 | .000815 | 1.0 |
| Nickel | 8.85 | .000242 | .000503 | .00214 | .00445 | 5.46 |
| Tantalum | 16.6 | 0.000068 | 0.000171 | 0.00113 | 0.00283 | 3.47 |

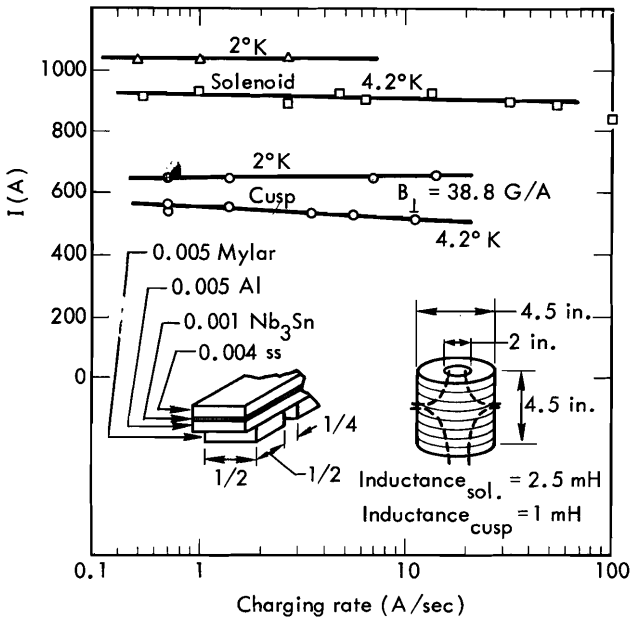


Fig. 3. Cryogenic stability of aluminum bonded $Nb_3Sn$.

adiabatic temperature rise of a strip with currents decaying from the full critical state can be found:

$$\Delta T \approx \frac{10^{-9}}{4} \frac{I_c^2}{CA} \ln\left(\frac{21}{w} + 1/2\right) ,$$

where $I_c$ is the critical current, C is the heat capacity per unit volume, and l, w, and A are the conductor length, width, and area, respectively. A calculation shows that it might be possible for this energy release to induce film boiling. This could have caused a complication, except that the recovery and peak heat fluxes are the same in the small insulation passages used.

## Aluminum Resistivity

To achieve high current densities with cryogenic stabilization, the resistivity of aluminum cladding must be extremely low. Below 10°K the Block-Grüneisen formula predicts that the intrinsic phonon resistivity of aluminum is negligible. Remaining, are the impurity resistivity of approximately 0.6 nΩ-cm/ppm[11] and the grain boundary resistivity of about 0.3 nΩ-cm.[12] Quantitatively, the result of lattice defects is unknown. Bulk resistivity ratios up to 45,000 have been reported in ultrapure aluminum.[13] However other complications, such as the size effect, magnetoresistance, and strain resulting from winding and thermal cycling make such resistivities unattainable in a magnet. Fickett has an excellent review of these resistive mechanisms in aluminum.[14] He suggests that size effect resistivity $\rho_s$ may be calculated from a simplified Fuch's equation:

$$\rho_s = \rho_b + \frac{(\rho l)_b}{d} ,$$

where $\rho_b$ is the bulk resistivity and d is the substrate thickness in centimeters. Values for the product of bulk resistivity times electronic mean free path $(\rho l)_b$ of 0.35 to 1.33 × $10^{-11}$ Ω-cm have been reported, but Fickett suggests using 0.7 × $10^{-11}$ Ω-cm in the liquid helium temperature range.[15]

Correlating the data of several others, Brown recommends the following formula for the lowest strain resistance[16]:

$$\rho_s = 110\ \varepsilon^{1.19} \times 10^{-9}\ \Omega\text{-cm} .$$

However, it seems that a simpler equation would be more appropriate to represent the average data:

$$\rho_s = 10^{-7}\ \varepsilon\ \Omega\text{-cm} .$$

The strain ε should include not only the strain under magnetic load, but also the strain from winding and the thermal strain from differential contraction of the aluminum, $Nb_3Sn$, and stainless steel. Thermal cycling of the magnet may further strain the aluminum alternately in compression and tension. Room-temperature tests indicate that the hardness increases during the first three strain cycles, then it remains constant. It is only speculation at this point that resistivity will behave similarly. If it does not, the

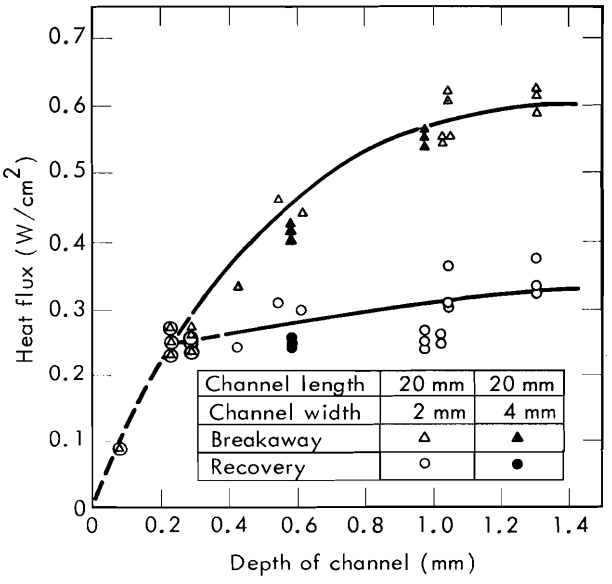


Fig. 4. Critical fluxes for vertical channels (from James, Lewis, and Maddock, Ref. 9).

aluminum would have to be periodically annealed by heating the entire magnet as high as 300°C for 1 hr. Perhaps, with sufficient strain and a longer time, the aluminum could be annealed at some lower temperature more compatible with the magnet insulation and solder joints.

Above resistivity ratios of 1000, Kohler's rule does not hold; that is, the effects of temperature are different than those of purity. In fact, the magnetoresistance peaks around 15 to 20°K, about four times greater than at 4.2°K.[15] Near liquid helium temperature, however, an empirical relation by Corruccini may be used for the magnetoresistance $\rho_H$[17]:

$$\frac{\rho_H}{\rho_\sigma} = \frac{H_*^2\ (1 + 0.00177\ H_*)}{1.8 + 1.6\ H_* + 0.53\ H_*^2}\ ,$$

where

$$H_* = H \cdot \frac{\rho_{300^\circ K}}{\rho_\sigma} \quad \text{(H is in megagauss)}\ .$$

Just what cooperative effects the size, strain, and magnetoresistance have on each other is not entirely clear. However, Stevenson[18] has noted that magnetoresistance is considerably more affected by strain than by purity. For similar reasons, Brown suggested that the strain resistivity $\rho_\sigma$ be used in the above magnetoresistance equation instead of the bulk resistivity.

One might expect that the size effect would be less important in a highly magnetic field, since the electrons would orbit, and not reach, the conductor boundaries despite a long electronic mean free path.[19] Especially when the magnetic field is applied perpendicular to the face of a tape, the Lorentz force causes the electrons to orbit in the wide plane. However, Sondheimer found (from the Boltzmann equation for free electrons) that the resistivity should oscillate with the field.[20] Increasing the field causes the oscillation to decrease in amplitude and to approach an asymptotic value:

$$\rho_{H \to \infty} = \rho_b + 3/8\ (1 - P)\ \frac{(\rho l)_b}{d}\ .$$

This effect has been observed by Försvoll and Holwech in aluminum.[21] Since the fraction of specularly scattered electrons P is generally unknown, this small correction can be ignored. Numerical calculations by summing the size effect and magnetoresistance agree with the data by Försvoll to within 25%. Considering all the other uncertainties in estimating strains and other cooperative effects, this procedure appears to be good enough for engineering estimating. The most important point regarding the size effects is that it does not diminish with increasing magnetic field, if the field is perpendicular to the face of the tape.

## Mechanical Properties

In large magnets, a concern of major importance is the structural properties of the superconductor. While high-purity aluminum is very soft and ductile, $Nb_3Sn$ is brittle, so that cladding the conductor with some high-strength, stiff material is necessary to enable it to withstand the large tensile loads. Stainless steel has often been used for this purpose. To predict the strength of such a composite conductor a method similar to that used by Benz[22] was adopted.[23] It was assumed that the elements of the laminated conductor are bonded at the soldering temperature. Cooling the conductor to 4°K causes a large residual compressive stress in the $Nb_3Sn$, because the aluminum and steel have larger coefficients of contraction. As a result, a considerable tensile force may be applied before straining the $Nb_3Sn$ in tension.

After bonding and cooling to 4°K, the initial strains in the steel, $Nb_3Sn$, and aluminum are as follows:

$$\varepsilon_{0ss} = (\varepsilon^*_{Al} - \varepsilon^*_{ss}) + \varepsilon_{0Al},$$

$$\varepsilon_{0Nb} = (\varepsilon^*_{Al} - \varepsilon^*_{Nb}) + \varepsilon_{0Al},$$

and

$$\varepsilon_{0Al} = \frac{E_{ss}V_{ss}(\varepsilon^*_{ss}-\varepsilon^*_{Al}) + E_{Nb}V_{Nb}(\varepsilon^*_{Nb}-\varepsilon^*_{Al}) - K_\sigma V_{Al}}{E_{Tan}V_{Al} + E_{ss}V_{ss} + E_{Nb}V_{Nb}}\ ,$$

where the symbols and representative values are given in Table II. By using the law of mixtures, the net modulus for the composite is calculated:

$$E_c = E_{ss}V_{ss} + E_{Nb}V_{Nb} + E_{Tan}V_{Al}\ .$$

Then the design stress $\bar{\sigma}_D$ on the total laminate can be found corresponding to the point at which $Nb_3Sn$ strain just reverses from compression to tension:

$$\bar{\sigma}_D = -\varepsilon_{0Nb}\ E_c\ .$$

A plot of design and failure stress is shown in Figs. 5 through 8 as a function of composition for two different bonding temperatures (solder solidus temperature). Fracture of the bare $Nb_3Sn$ occurs at about 0.2% strain; but when bonded, the fracture strain increases to 0.3% because of the initial biaxial compressive stresses producing lateral constraint. This fracture strain was measured by supplying near-critical current to a short sample of composite conductors in a 75 kG field and straining the conductor to failure of the $Nb_3Sn$ layer. A summary of these tests is shown in Table III.

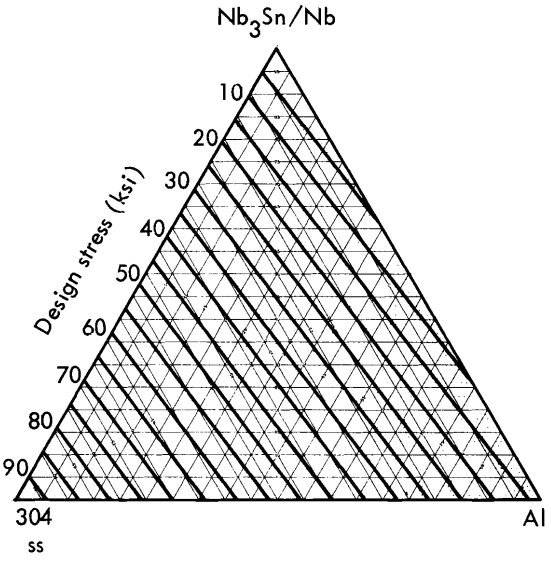


Fig. 5. Design stress as a function of composition (not corrected for solder volume; solder solidus ~183°C).

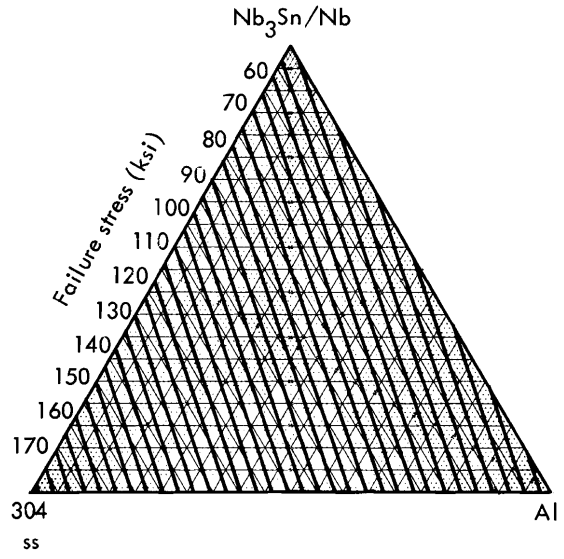


Fig. 6. Failure stress as a function of composition (not corrected for solder volume; solder solidus ~183°C).

In tension, high-purity aluminum yields below a few thousand psi stress, causing a resistance increase. Still, the large bearing pressures in a magnet winding may be supported, if the soft aluminum is used in thin strips and bonded to a strong substrate. Such a configuration produces a hydrostatic stress condition in which the bearing strength approaches that of the substrate. However, when interrupting the interlayer insulation for face cooling of the superconductor, stress concentrations lower the bearing strength. In fact, at 4.2°K, aluminum under a 0.25-in. roller was found to yield immediately under load and cause a resistance increase. Other flat insulations, such as a 0.125-in.-wide strip of Mylar on a 0.375-in. conductor, caused yielding at 5850 psi. Increasing the conductor width to 0.75-in. while keeping the insulation width the same, increased the allowable bearing stress to greater than 9000 psi.

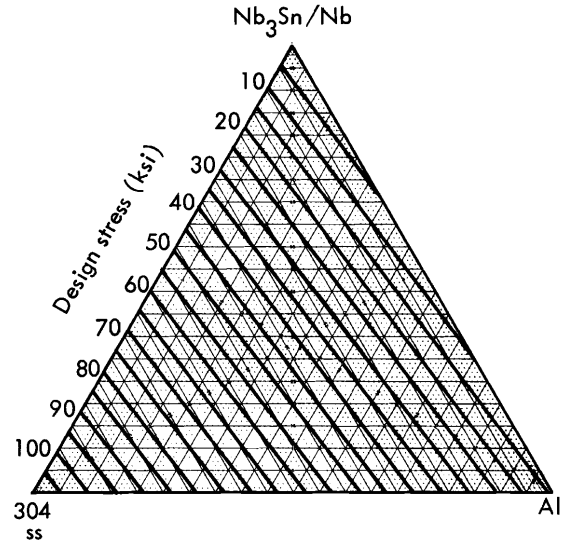


Fig. 7. Design stress as a function of composition (not corrected for solder volume; solder solidus ~233°C).

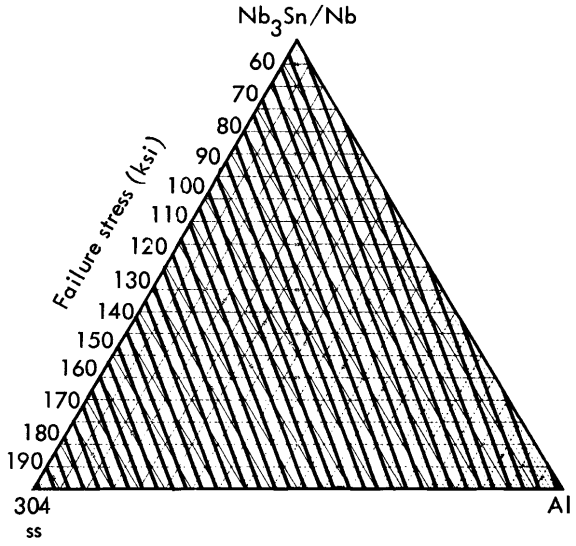


Fig. 8. Failure stress as a function of compositior (not corrected for solder volume; solder solidus ~233°C).

TABLE II. Representative Material Parameters

| Symbol | Meaning | Value at 4.2°K for 60-40 Sn-Pb solder |
|---|---|---|
| $E_{ss}$ | Young's modulus for stainless steel | $29 \times 10^6$ psi |
| $E_{Nb}$ | Young's modulus for $Nb_3Sn$ | $17 \times 10^6$ psi |
| $E_{Tan}$ | Tangent modulus for aluminum | $1.2 \times 10^6$ psi |
| $E^*_{ss}$ | Thermal contraction for stainless steel | $-5.86 \times 10^{-3}$ |
| $E^*_{Nb}$ | Thermal contraction for $Nb_3Sn$ | $-2.60 \times 10^{-3}$ |
| $E_{Al}$ | Thermal contraction for aluminum | $-8.13 \times 10^{-3}$ |
| $K_\sigma$ | Idealized yield stress of aluminum | $6.2 \times 10^3$ psi |
| $V_{ss}$ | Vol% stainless steel | |
| $V_{Nb}$ | Vol% $Nb_3Sn$ | |
| $V_{Al}$ | Vol% aluminum | |

TABLE III. Summary of Fracture Test Experiments

| Conductor composition | | | | | Solder solidus temp. °C | Design stress calculated psi | Failure stress calculated psi | Failure stress experimental psi |
|---|---|---|---|---|---|---|---|---|
| Thickness in. | $V_{Al}$ | $V_{ss}$ | $V_{Nb}$ | $V_{sol}$ | | | | |
| 0.00115 | 0.435 | 0.348 | 0.087 | 0.130 | 183 | 38,400 | 74,800 | 74,800 |
| 0.00115 | 0.435 | 0.348 | 0.087 | 0.130 | 233 | 44,500 | 81,000 | 82,500 |
| 0.0185 | 0.540 | 0.217 | 0.108 | 0.135 | 233 | 38,500 | 58,000 | 60,300 |
| 0.0200 | 0.500 | 0.200 | 0.150 | 0.150 | 233 | 29,000 | 55,900 | 63,000 |

Another consequence of face cooling is local bending resulting from misalignment of the insulation strips on the two faces of the conductor. The composite conductor must have sufficient beam strength to prevent yielding. Accordingly, the steel must be on the outside of the composite where the bending stresses are the highest, and the solder must have good shear strength with reasonable ductility. High-lead solders are sufficiently strong and have good ductility.[24] An added advantage of the high-lead solders is the relatively high melting temperature, which increases the initial compression of the $Nb_3Sn$ and allows greater stress in the steel.

TABLE IV. Properties of Some Stiff Materials

| Material | Young's mod $10^6$ psi | Crystal structure | Resistance 270°K μΩ-cm | Thermal conductivity cal/sec-°C cm |
|---|---|---|---|---|
| Beryllium | 37 | HCP | 5.9 | 0.38 |
| Chromium | 36 | BCC | 13 | 0.16 |
| Cobalt | 30 | HCP | 6.24 | 0.165 |
| Iridium | 75 | FCC | 5.3 | 0.14 |
| Iron | 28.5 | BCC | 9.71 | 0.18 |
| Molybdenum | 50 | BCC | 5.17 | 0.35 |
| Nickel | 30 | FCC | 6.84 | 0.22 |
| Osmium | 80 | HCP | 9.5 | |
| Rhodium | 42 | FCC | 4.5 | 0.21 |
| Tantalum | 27 | BCC | 12.4 | 0.13 |
| Tungsten | 50 | BCC | 5.5 | 0.48 |
| Boron filaments | 120 | Amorphous | | |
| Carbon filaments | 100 | Amorphous | Variable | |

## Conclusion

Aluminum bonded $Nb_3Sn$ is a reasonable conductor for large fusion magnets. The problems of winding a brittle strip in a multiaxis configuration are being resolved[25] and overall current densities of 7000 A/cm at 120 kG are achievable with cryogenic stability. If the aluminum bond can be improved, dynamic stabilization may be able to permit still higher current densities in high radial fields. Yet, since an occasional fracture of the $Nb_3Sn$ seems inevitable in a large magnet (measured losses around 1 W per crack suggest that several such fractures could be allowed), cryogenic stability is most likely to ensure successful operation of large, high-field magnets.

## References


1. C. D. Henning, R. L. Nelson, M. O. Calderon, A. K. Chargin, A. R. Harvey, and B. S. Denhoy, "Large Superconducting Baseball Magnet — Part II," in Proc. XIII, Int. Conf. of Refrig. (1971).
2. Intermagnetics General Corp., Schenectady, New York.
3. D. L. Coffey, W. F. Gauster, and M. S. Lubell, J. Appl. Phys. 42, 1 (1971).
4. R. Hancox, in Proc. Inter. Conf. Magnet Technology, 3rd Hamburg (1970), p. 950.
5. C. P. Bean, Phys. Rev. Letters 8, 6 (1962).
6. P. S. Swartz and C. P. Bean, J. Appl. Phys 39, (1968), 4991.
7. H. R. Hart, "Magnetic Instabilities and Solenoid Performance: Applications of the Critical State Model," in Proc. of Summer Study on Superconducting Devices and Accelerators, BNL (1968), pp. 571-600.
8. R. Hancox, "Review of Stabilization Techniques," in Proc. of Conf. on Fusion Reactor Technology, ORNL (1971), pp. 296-302.
9. G. R. James, K. G. Lewis, and B. J. Maddock, Cryogenics 11, 7 (1971).
10. F. W. Grover, Inductance Calculations: Working Formulas and Tables (Dover, New York, 1962).
11. M. B. Kasen, NBS, Boulder, Colo., private communication.
12. M. B. Kasen, Phil. Mag. 21, 171 (1970).

13. V. D. Arp, M. B. Kasen, and R. P. Reed, "Magnetic Energy Storage and Cryogenic Aluminum Magnets," Air Force Aeropropulsion Laboratory Technical Report AFAPL-TR-68-67 (1969).

14. F. R. Fickett, Cryogenics 11, 5 (1971).

15. F. R. Fickett, Phys. Rev. B 3, 6 (1971).

16. G. V. Brown, "High-Field Cryogenic Magnets with Pure Aluminum Conductor," NASA Tech. Memo. X-52571 (1969).

17. R. J. Corruccini, "The Electrical Properties of Aluminum for Cryogenic Electromagnets," NBS Tech. Note No. 218, Boulder, Colo., (1964).

18. R. Stevenson, Canadian J. Phys. 45, 12 (1967).

19. G. Brändli and J. L. Olsen, Mater. Sci. Eng. 4, 2 (1969).

20. E. H. Sondheimer, Phys. Rev. 80, 3 (1950), p. 401.

21. K. Försvoll and I. Holwech, Phil. Mag. 9, 99 (1964).

22. M. G. Benz, J. Appl. Phys. 39, 6 (1968).

23. H. L. Leichter, "Mechanical Properties of Composite $Nb_3Sn$ Superconductors" (to be published).

24. A. B. Kaufman, Des. Eng. 48, 6 (1958).

25. A. R. Harvey, "A Winding Technique for Superconducting Tape in Multi-Axis Magnets," this conference.